# Xanthan Stability at Elevated Temperatures

R.S. Seright,* SPE, and B.J. Henrici, Exxon Production Research Co.

**Summary.** Xanthan stability is examined to define more clearly the polymer's temperature limitations as a mobility-control agent. Experiments were performed to probe the relative importance of hydrolysis, oxidation, and helix-coil transitions in xanthan degradation. In the absence of oxidizing agents (i.e., dissolved oxygen), results indicate that free-radical, oxidation/reduction reactions are not the dominant mechanism for xanthan degradation. Depending on the pH, acid-catalyzed hydrolysis and base-catalyzed fragmentation reactions may play important roles. With Arrhenius calculations, it was estimated that under ideal conditions (no dissolved oxygen, pH 7 to 8, and moderate to high salinities), a xanthan solution could maintain at least half of its original viscosity for a period of 5 years if the temperature does not exceed 75 to 80°C [167 to 176°F]. New polymers will be needed for chemical floods where xanthan does not have sufficient stability.

## Introduction

About **50%** of the oil in the **U.S.** that could be recovered by chemical flooding exists in reservoirs that have temperatures above **60°C** [140°F].[1] Stable, water-soluble polymers will generally be required during these floods to provide mobility control. Much progress has been made toward understanding the temperature limitations of acrylamide-based polymers—particularly in brines that contain divalent cations.[2-6] However, there is still considerable uncertainty about the stability of xanthan solutions at elevated temperatures.

The goal of this work is to define more clearly the limits of stability for xanthan at elevated temperatures in the absence of dissolved oxygen. This paper first summarizes the known composition and structure of xanthan. Second, the literature is examined to review those types of mechanisms that could contribute to chemical cleavage of the xanthan-polymer backbone during long-term exposure to reservoir conditions. Next, techniques are briefly described for preparing, monitoring, and maintaining solutions with undetectable concentrations of dissolved oxygen (< 2 ppb). Results are reported for experiments that probe the relative importance of hydrolysis, oxidation, and helix/coil transitions in xanthan degradation. Finally, temperature limitations associated with the use of xanthan as a mobility-control agent are discussed.

## Xanthan Composition and Structure

Fig. 1 illustrates the chemical composition[7] of xanthan. The backbone of the molecule is composed of glucose monomers connected by $\beta$(1-4) gycosidic linkages. A side chain that contains the trisaccharide sequence mannose/glucuronic-acid/mannose is attached to every other glucose residue in the backbone. In each side chain, an 0-acetyl group is usually bound to the mannose residue closest to the main chain of the polymer. Some of the terminal mannose units in the side chains may contain a ketal-linked pyruvate group. Depending on the bacterial strain producing the polymer, the fraction of side chains containing pyruvate may be **0%**, 100%, or some intermediate value.[7-11].

Weight-average molecular weights reported for native xanthan samples have ranged from 2 million to 50 million daltons.[12-16] Most of the molecular weight values are in the low end of this range. Polydispersity indexes ($M_w/M_n$) between 1.4 and 2.8 have been published.[13-15] The radius of gyration of native xanthan has been estimated to be between 0.1 and 0.4 $\mu$m in saline solutions.[16,17] Xanthan has been modeled as a rigid-rod molecule whose length is between 0.6 and 1.5 $\mu$m[14,16] and whose diameter is about 2 nm [20 Å].[16,18,19] Because the contour length of xanthan is thought to be in the range of 2 to **10** $\mu$m,[15,18] the molecule is presumed to have some flexibility rather than being strictly a rigid rod.[14,20,21] Consequently, xanthan has also been modeled as a worm-like chain whose persistence length is between 50 and 120 nm [500 and 1,200 Å].[20,22,23] The rigidity of native xanthan is attributed to the helical structure of the molecule. Some researchers have argued that the xanthan helix is composed of a single polysaccharide strand,[15,19,22] while others regard xanthan as a double-stranded helix.[13,17] Still other researchers suggest that xanthan can assume different ordered configurations (including single- and double-stranded helixes) depending on salinity, temperature, and sample history.[11,24]

## Xanthan Reactions and Degradation Mechanisms

**Helix/Coil Transition.** Xanthan is capable of undergoing a helix/coil transition (or perhaps more correctly, an "order/disorder" transition) as temperature is increased.[25,26] In aqueous solutions of very low salinity, this transition can occur near room temperature. The transition or "melting" temperature, $T_m$, increases in direct proportion to the logarithm of the salt concentration. The following formula, based on the data of **Holzwarth**,[25] relates $T_m$ to the molar sodium concentration, [Na$^+$]:

$$T_m = 122 + 30 \log[\mathrm{Na}^+]. \qquad (1)$$

For comparison, the data of Milas and **Rinaudo**[26,27] can be described by use of

$$T_m = 125 + 43 \log[\mathrm{Na}^+]. \qquad (2)$$

The melting temperature is much more sensitive to divalent cations than to monovalent cations. Eq. 3, which is based on Holzwarth's data, quantifies the effect of molar calcium concentration, [Ca$^{++}$], on $T_m$:

$$T_m = 310 + 70 \log[\mathrm{Ca}^{++}]. \qquad (3)$$

The melting temperature can be influenced by the acetate and pyruvate contents of the xanthan.[28] Even so, $T_m$ is expected to be quite high for the salinity and hardness levels that are characteristic of most formation brines. For example, in a 3 wt% NaCl solution, $T_m$ is estimated to be 113°C [235°F] with either Eq. **1 or** 2. The presence of calcium raises the melting temperature dramatically. In a **0.3** wt% $CaCl_2$ brine, Eq. **3** predicts a value of 200°C **[392°F]** for $T_m$.

Xanthan stability at elevated temperatures is much greater in saline solutions than in deionized water.[27] The helical conformation of xanthan in saline solutions is thought to protect the molecule from chain scission. In low-salinity solutions, however, xanthan will be in the disordered, coil conformation and, therefore, may be much more susceptible to chemical attack. A key question is whether helix/coil transitions are important during xanthan degradation in saline solutions.

**Oxidation.** **Wellington**[29] discussed the role of free-radical, oxidative/reductive reaction mechanisms in xanthan degradation. These mechanisms require the presence of an oxidizing agent—usually molecular oxygen. Molecular oxygen can react to form hydroxyl and peroxide radicals that can play a major role in the degradation of polysaccharides.[30,31] To minimize xanthan degradation from these mechanisms, **Wellington**[29] proposed the use of an antioxidant formulation containing (1) a free-radical transfer agent (e.g.,

---

*Now at New Mexico Petroleum Recovery Research Center

## TABLE 3—VAPOR-PHASE COMPOSITION FOR HYDROCARBON-EXTRACTION EXPERIMENTS

**$CO_2$ at 122°F and 1,400 psi**

| Time (minutes) | Vapor-Phase Composition (mole fraction) | | | |
|---|---|---|---|---|
| | $CO_2$ | $C_{10}$ | $C_{12}$ | $C_{16}$ |
| 0 | 1.0000 | 0.0000 | 0.0000 | 0.0000 |
| 60 | 0.9910 | 0.0053 | 0.0024 | 0.0013 |
| 120 | 0.9884 | 0.0069 | 0.0031 | 0.0016 |
| 180 | 0.9879 | 0.0073 | 0.0032 | 0.0017 |
| 220 | 0.9878 | 0.0074 | 0.0032 | 0.0017 |
| 1,200 | 0.9877 | 0.0074 | 0.0032 | 0.0017 |
| 1,435 | 0.9875 | 0.0076 | 0.0032 | 0.0016 |

**$CO_2$/Entrainer at 122°F and 1,400 psi**

| Time (minutes) | Vapor-Phase Composition (mole fraction) | | | | |
|---|---|---|---|---|---|
| | $CO_2$ | $iC_8$ | $C_{10}$ | $C_{12}$ | $C_{16}$ |
| 0 | 0.9204 | 0.0796 | 0.0000 | 0.0000 | 0.0000 |
| 65 | 0.9525 | 0.0370 | 0.0064 | 0.0031 | 0.0011 |
| 125 | 0.9496 | 0.0336 | 0.0093 | 0.0051 | 0.0024 |
| 160 | 0.9469 | 0.0303 | 0.0121 | 0.0071 | 0.0035 |
| 220 | 0.9478 | 0.0261 | 0.0133 | 0.0087 | 0.0041 |
| 1,300 | 0.9466 | 0.0255 | 0.0141 | 0.0093 | 0.0045 |
| 1,360 | 0.9467 | 0.9255 | 0.0141 | 0.0092 | 0.0045 |

from 1,800 to 3,200 psia [12.4 to 22.1 MPa]. The results showed no significant viscosity increase at pressures below 3,200 psia [22.1 MPa]. The maximum viscosity increase was about ***50%*** at these conditions.

The results of the screening tests showed only limited solubility of ndecanol and the ethoxylated alcohol in supercritical $CO_2$. This limited solubility resulted in minimal improvement in gas-phase viscosity and density when these cosolvents were tested at the experimental conditions. Isooctane and 2-ethylhexanol, on the other hand, showed gas-phase viscosity enhancement when appreciable cosolvent dissolved into the $CO_2$-rich phase.

Experiments were also performed to compare the effects of $CO_2$ and cosolvent on heavy-hydrocarbon gas-phase solubility. The 2,2,4-trimethylpentane (isooctane) and 2-ethylhexanol were selected because of the potential exhibited by these additives in increasing the solution gas-phase viscosity when operating close to the mixture's critical pressure.

The study with isooctane was performed at 122°F and 1,400 psia [50°C and 9.7 MPa]. The synthetic oil used for the extraction experiment was an equal-volume mixture of n-decane, n-dodecane, and n-hexadecane. Table 3 presents the results of the experiments comparing $CO_2$ alone and $CO_2$ plus isooctane. Table 3 also shows the vapor-phase mole fractions for the two extraction modes. Fig. 8 shows the changes of vapor-phase component distribution (mole fraction) as a function of time. The results indicated an increase in the total amount of extracted hydrocarbons into the vapor phase and an enrichment in n-dodecane and n-hexadecane extraction when the cosolvent was added to the system. The results clearly indicate that heavy-component selectivity was promoted and, at the same time, an increase in overall oil extraction was achieved in the presence of the cosolvent.

## Conclusions

1. The presence of entrainers (cosolvents) that have appreciable solubility in the $CO_2$ phase effectively increased the viscosity and density of the gas phase.
2. The presence of cosolvents in $CO_2$ effectively increased the solubility of the components of hydocarbon mixtures into the $CO_2$-rich phase.
3. Operating at pressure regions beyond the critical pressure of the mixture, at a given temperature, and varying the concentration of the cosolvent in the mixture resulted in significant changes in fluid viscosity. Although adding more of certain cosolvents can increase $CO_2$-rich-phase density and viscosity, an optimum concentration of cosolvent to use will exist that will be dictated by economic evaluation and reservoir simulation of the process.
4. The selection of candidate cosolvents should depend on the reservoir conditions encountered. At the experimental temperatures tested, 104 and 122°F [40 and 50°C], different cosolvents showed different pressure regions where fluid-property enhancement occurred.

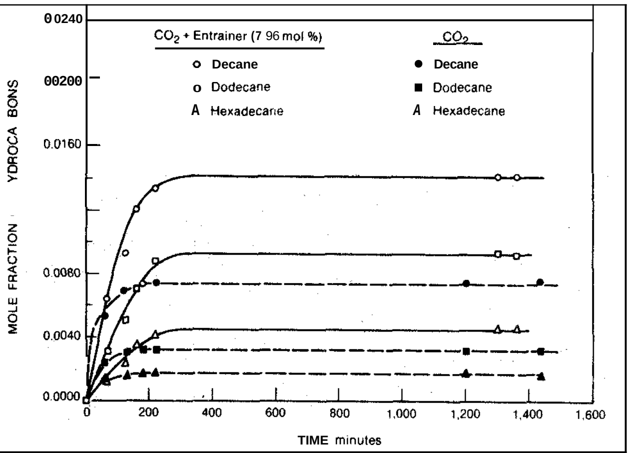

Fig. 8—Component extraction with $CO_2$ and $CO_2$ plus isooctane at 50°C and 96.5 bars.

## Acknowledgment

This work was sponsored by the **U.S.** DOE under cooperative agreement DE-FC22-83-FE60149.

## References

1. Gardner, J.W., Orr, F.M. **Jr.**, and Patel, P.D.: "The Effect of Phase Behavior on $CO_2$ Flood Displacement Efficiency," JPT (Nov. **1981) 2067–81.**
2. Orr, F.M. Jr., Yu, A.D., and Lein, C.L.: "Phase Behavior of $CO_2$ and Crude Oil in Low Temperature Reservoirs," ***SPEJ*** (Aug. **1981) 480–92.**
3. Holm, L.W. and Josendal, V.A.: "Effect of Oil Composition on Miscible-Type Displacement by Carbon Dioxide," ***SPEJ*** (Feb. **1982) 87–98.**
4. Heller, J.P. ***et al.:*** "Direct Thickeners for Mobility Control of $CO_2$ Floods," ***SPEJ*** (Oct. **1985) 679–86.**
5. Dandge, D.K. and Heller, J.P.: "Polymers for Mobility Control in $CO_2$ Floods," paper SPE **16271** presented at the **1987** SPE Intl. Symposium on Oilfield Chemistry, San Antonio, Feb. **4–6.**
6. Terry, R.E. ***et*** al.: "Polymerization in Supercritical $CO_2$ To Improve $CO_2$/Oil Mobility Ratios," paper SPE **16270** presented at the **1987** SPE Intl. Symposium on Oilfield Chemistry, San Antonio, Feb. 4–6.
7. Peter, S., Brunner, G. and Riha, R.: "Zur Trennung schwerfliichtiger Stoffe mit Hilfe fluider Phasen," Monograph **73,** DECHEMA **(1974).**
8. Brunner, G.: "Selectivity of Supercritical Compounds and Entrainers with Respect to Model Substance," ***Fluid*** Phase ***Equilibria*** **(1983) *10,* 289.**
9. Joshi, D.K. and Prausnitz, J.M.: "Supercritical Fluid Extraction with Mixed Solvents," ***AIChE*** **J. (1984) 30,** No. **3, 522–25.**
10. Walsh, J.M., Ikonomou, G.D., and Donohue, M.D.: "Supercritical Phase Behavior: The Entrainer Effect," ***Fluid*** Phase ***Equilibria*** **(1987) 33, 295–314.**
11. Schmitt, W.J. and Reid, R.C.: "The Use of Entrainers in Modifying the Solubility of Phenanthrene and Benzoic Acid in Supercritical Carbon Dioxide and Ethane," ***Fluid*** Phase ***Equilibria*** **(1986) *32,* 77–99.**
12. Cullick, **A.S.:** "Enhanced Oil Recovery Using Carbon Dioxide," U.S. Patent No. **4,609,043** (Sept. **1986).**
13. **Prausnitz,** J.M. and Benson, P.R.: "Solubility of Liquids in Compressed Hydrogen, Nitrogen, and Carbon Dioxide," ***AIChE*** J. **(1959) *5,* No. 2, 161–64.**
14. Peng, D.Y. and Robinson, D.B.: "A New Two-Constant Equation of State," *Ind.* ***& Eng. Chem. Fund.*** **(1976) 15, No. 59, 59–64.**

## SI Metric Conversion Factors

| | | | | |
|---|---|---|---|---|
| bar | × 1.0* | E+05 | = | Pa |
| cp | × 1.0* | E−03 | = | Pa·s |
| °F | (°F−32)/1.8 | | = | °C |
| psi | × 6.894 757 | E+00 | = | kPa |

*Conversion factor is exact.

**SPERE**

Original SPE manuscript received for review March 22, 1988. Paper accepted for publication May 31, 1989. Revised manuscript received May 8, 1989. Paper (SPE 17344) first presented at the 1988 SPE/DOE Enhanced Oil Recovery Symposium held in Tulsa, April 17–20.

thiourea); (2) a “sacrificial,” easily oxidizable alcohol; (3) an oxygen scavenger; and (4) a ‘‘sufficient’’ brine concentration. Several other formulations and chemical additives have been proposed to protect xanthan from oxidative degradation, including aliphatic alcohols,[32] amines,[33,34] and iodides.[35]

Our field results indicated that dissolved oxygen is generally absent from water produced from oil reservoirs. Furthermore, it is common that fluids injected during waterflood and EOR operations contain little, if any, dissolved oxygen. Therefore, another important question is whether oxidative reactions constitute the dominant degradation mechanism for xanthan in the absence of oxygen.

It has been suggested that peroxides may be generated in xanthan broths because of extensive aeration during fermentation.[36] If this is correct, these peroxides could conceivably cause some oxidative degradation even if the polymer is injected under anaerobic conditions. To counter this possibility, use of reducing agents, such as sodium borohydride, has been proposed to destroy peroxides in xanthan formulations.[36]

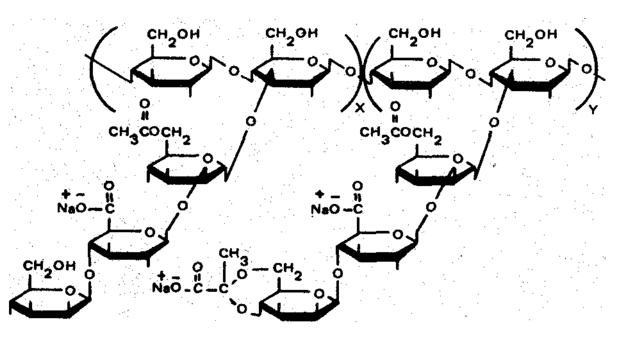

Fig. 1—Xanthan chemical composition.

Hydrolysis. Many of the bonds in the xanthan molecule are subject to cleavage by hydrolysis. The acetyl groups have long been recognized to be very susceptible to base-catalyzed hydrolysis.[37] Ash et *al.*[38] estimated the half-life for acetyl groups on xanthan to be 130 days at 60°C [140°F] and pH 6. They also found that the half-life decreases sharply as temperature or pH is increased. Thus, for a chemical flood in which xanthan is exposed to temperatures above 60°C [140°F] for several years, the polymer could be virtually acetate-free during most of the flood. Reports vary on the effects of deacetylation on xanthan properties. Some researchers[39] find that deacetylation has little effect on xanthan properties, while others[37] find that the viscosity of a xanthan solution changes significantly upon deacetylation.

After the O-acetyl groups, the pyruvate-ketals in xanthan are the next most labile groups at neutral pH. Acid-catalyzed hydrolysis is the principal pathway for removal of pyruvate from xanthan.[40,41]

The glycosidic linkages between sugar units are also susceptible to hydrolysis. Hot-acid treatment is a common method used to hydrolyze polysaccharides into their constituent sugars. Eq. 4 represents the reaction for acid-catalyzed hydrolysis of cellobiose [a disaccharide consisting of two *β*(1-4) linked glucose units], which contains the same linkage present in the backbone of xanthan:

$$\text{glucose}-\text{glucose}+\text{H}_2\text{O} \xrightarrow{\text{H}^+} 2\ \text{glucose}. \quad \ldots\ldots\ldots\ldots\ldots\ldots (4)$$

In a review of acid-catalyzed hydrolysis of polysaccharides, BeMiller[42] reported first-order rate constants for the reaction in Eq. 4 to be on the order of $10^5$ seconds$^{-1}$ in strong acids (e.g., 0.1 *N* HCl). Also, the activation energy for hydrolysis was reported to be about 125 kJ/mol [118 Btu/mol] between 60 and 100°C [140 and 212°F]. Of course, acid-catalyzed hydrolysis of glycosidic linkages will be much slower as pH increases. Unfortunately, we are not aware of any studies of polysaccharide hydrolysis that have been conducted at neutral pH. It is conceivable that hydrolysis may still be an important degradation mechanism considering the long time periods that xanthan will be exposed to the reservoir temperature.

Although polysaccharides are generally more stable in bases than in acids, they are susceptible to a number of base-catalyzed fragmentation reactions.[41] An example is

$$\text{glucose-glucose} \xrightarrow{\text{OH}^-} \text{glucose}+\text{isosaccharinic acid.} \quad \ldots\ldots (5)$$

In addition to acid- and base-catalyzed reactions, it is also possible that water molecules, chloride, and other anions promote hydrolysis of glycosidic linkages through nucleophilic substitution.[43]

Knowing the relative importance of the various types of degradation mechanisms under anticipated reservoir conditions (low oxygen content, neutral pH, moderate-to-high salinity) would be helpful. This knowledge would allow more productive efforts to maximize xanthan stability and provide a better understanding of the upper temperature limit for xanthan use. Thus, attaining an improved knowledge of the nature of xanthan degradation and the limits of xanthan stability is a goal of this investigation. It is not within the scope of this work, however, to establish the exact, detailed mechanisms for xanthan degradation. To do so would require an extensive analysis of all degradation products as well as determination of molecular weight distributions during degradation.

## Experimental

Xanthans from four different commercial sources were used. Xanthans A, C, and D were supplied as broths that contained between 4 and 8% active polymer. Xanthan B was supplied as a powder. Solutions were mixed inside an anaerobic chamber. The remaining oxygen normally was eliminated by addition of a chemical oxygen scavenger (e.g., 500 ppm $\text{Na}_2\text{S}_2\text{O}_4$). Sulfite/oxygen reactions and reaction rates are known to vary with temperature, pH, and salinity of the aqueous solvent.[44] We rely on dissolved oxygen measurements to confirm that dissolved oxygen levels below 2 ppb are achieved and maintained throughout the course of our experiments. Dissolved oxygen content in solutions was measured with the CHEMet™ colorimetric technique marketed by Chemetrics Inc. A detailed description of the experimental procedure is included in Ref. 45.

Viscosity, pH, and dissolved oxygen content were routinely monitored during each stability test. In addition, solutions were checked visually for color, clarity, and formation of gels and precipitates. For a few key solutions, samples were examined for microbial growth. Only trace remnants of nonmotile *Xanthomonas* bacteria were found. No other microorganisms were detected.

Table 1 is a typical data set from a stability study. Viscosities were measured at five different shear rates ranging from 1.75 to 69.5 seconds–‘. For the data associated with each shear rate, a least-squares regression was performed to judge how well viscosity, *μ*, vs. time, *t*, could be described using the simple exponential decay model:

$$\ln[(\mu-\mu_s)/(\mu_o-\mu_s)]=-t/\tau, \quad \ldots\ldots\ldots\ldots\ldots\ldots\ldots\ldots (6)$$

where $\mu_s$ = solvent viscosity and $\mu_o$ = initial viscosity of the polymer solution. Decay constants, *τ*, and correlation coefficients, *r*, from the regression are listed at the bottom of each viscosity column. As other researchers[4] have noted, the decay constants tend to be greater when viscosities are monitored at high shear rates. For the example in Table 1, the decay constant at 69.5 seconds–’ is more than twice that at 1.75 seconds–’. Throughout the remainder of this paper, only viscosity values at 11 seconds$^{-1}$ will be reported, even though viscosities at the other four shear rates are also available. Also, because of the large amount of data collected, generally only the decay constant or the viscosity half-life will be for a given experiment. Unless Stated Otherwise, the dissolved Oxygen levels were maintained at an undetectable level (<2 ppb) throughout each stability study, regardless of the pH, salinity, or storage temperature of the solution.

## Results and

**pH Effects.** Unbuffered xanthan solutions exhibit a pH drop when exposed to elevated temperatures. At 96 and 120°C [205 and

TABLE 1—1,500 ppm XANTHAN A, 3% NaCl, 0.3% $CaCl_2$ STORED IN A GLASS CONTAINER AT 96°C, NO OXYGEN SCAVENGER USED

| | Viscosity at 25°C (mPa·s) | | | | | | |
|---|---|---|---|---|---|---|---|
| Day | 1.75 seconds$^{-1}$ | 4.4 seconds$^{-1}$ | 11 seconds$^{-1}$ | 27.7 seconds$^{-1}$ | 69.5 seconds$^{-1}$ | $O_2$ (ppb) | pH |
| 0 | 139.9 | 90.8 | 53.6 | 29.9 | 16.7 | <2 | 7.14 |
| 0.7 | 120.5 | 81.6 | 50.2 | 28.7 | 16.3 | — | 5.54 |
| 2 | 114.5 | 79.1 | 49.1 | 28.4 | 16.2 | — | 5.00 |
| 4 | 105.9 | 74.9 | 47.7 | 27.9 | 16.0 | <2 | 4.90 |
| 6 | 102.6 | 73.1 | 46.8 | 27.7 | 16.0 | — | 4.90 |
| 13 | 81.7 | 61.4 | 41.1 | 25.2 | 15.0 | — | 4.80 |
| 16 | 83.6 | 63.2 | 42.3 | 26.0 | 15.4 | — | 4.77 |
| 27 | 65.3 | 52.0 | 36.6 | 23.4 | 14.4 | — | 4.80 |
| 36 | 55.6 | 45.6 | 33.1 | 22.0 | 13.6 | <2 | 4.68 |
| 51 | 37.7 | 33.6 | 26.3 | 18.7 | 12.2 | — | 4.70 |
| 65 | 31.7 | 28.5 | 23.1 | 17.0 | 11.4 | — | 4.83 |
| 82 | 21.9 | 20.9 | 18.1 | 14.2 | 10.0 | <2 | 4.72 |
| 96 | 17.3 | 16.8 | 15.1 | 12.5 | 9.4 | — | 4.80 |
| 110 | 11.6 | 11.5 | 10.8 | 9.4 | 7.6 | — | 4.80 |
| 124 | 7.4 | 7.5 | 7.3 | 6.9 | 6.0 | <2 | 5.03 |
| 138 | 5.6 | 5.6 | 5.6 | 5.4 | 4.9 | — | 4.77 |
| 152 | 3.9 | 4.0 | 4.1 | 4.1 | 3.9 | — | 4.80 |
| 166 | 3.3 | 3.4 | 3.3 | 3.3 | 3.3 | ≤2 | 4.80 |
| $\tau$, days | 46 | 52 | 63 | 81 | 112 | pH: | 4.81 |
| $r$ | 0.998 | 0.996 | 0.992 | 0.984 | 0.977 | | |

248°F], most of the decline in pH occurs within the first day at the elevated temperature. Thereafter, very little additional pH drop is observed (Fig. 2). This decline in pH is attributable to hydrolysis of 0-acetyl groups (Ac) from xanthan (R):

$$R\text{-}Ac+H_2O \rightarrow R\text{-}OH+Ac^-+H^+ \quad \ldots\ldots\ldots\ldots\ldots\ldots (7)$$

In Fig. 2, the pH drop over 40 days was less at 64 and 80°C [147 and 176°F] than at the higher temperatures. However, the pH did continue *to* decline gradually at the two lower temperatures. To reach pH 5.8 required 162 days at 80°C [176°F] and 307 days at 64°C [147°F]. The time and temperature dependencies of the pH drop are consistent with the kinetics of acetyl-group hydrolysis reported by Ash et *al.*[38]

In the absence of dissolved oxygen, the time dependence of viscosity losses for xanthan solutions can usually be described quite well with an exponential decay model (Eq. 6). The linearity of the first-order kinetic plots in Fig. 3 illustrates this point for xanthans from three different commercial sources. It is somewhat fortuitous that the viscosity-loss curves *can* be characterized by single exponentials. This could not have been predicted in advance without a detailed knowledge of (1) the kinetics of bond cleavage, (2) the variation of the polymer molecular weight distribution during degradation, and (3) the relationship between molecular weight distribution and viscosity.

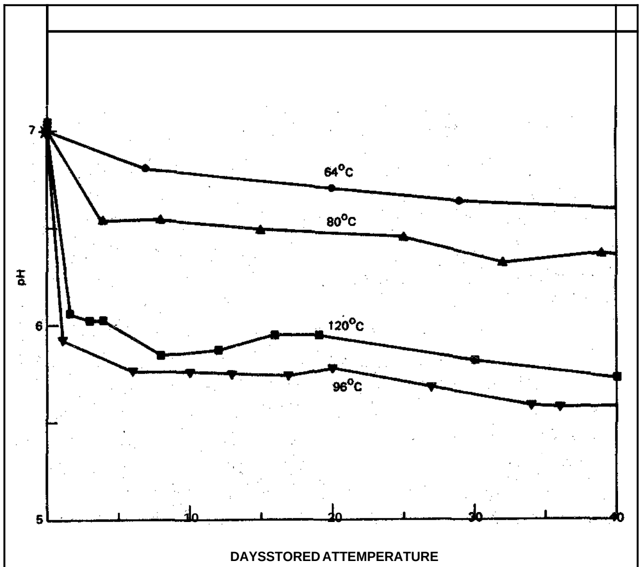

**Fig. 2—pH drop in unbuffered solutions: 1,500 ppm Xanthan B, 3% NaCl, 0.3% $CaCl_2$, 500 ppm $Na_2S_2O_4$, <2 ppb $O_2$.**

In Fig. 3, the value of $(\mu-\mu_s)/(\mu_o-\mu_s)$ for each of the three polymers is defined as equal to 1.0 at the beginning of the experiment. Note, however, that the y-intercept values from the linear regressions are different for the three polymers. The intercept value associated with Xanthan B (1.0) indicates that short-term exposure (1 day) to 120°C [248°F] has little effect on the viscosity of this polymer solution. As discussed above and in Ref. 38, the principal short-term chemical reaction is hydrolysis of acetyl groups. Thus, our findings for this polymer are consistent with the observation made by McNeely and Kang[39] that deacetylation has little effect on its solution properties. In contrast, the solution of Xanthan D exhibits a 70% viscosity increase during the first day at 120°C [248°F]. This behavior is consistent with the findings of Jeanes et al.[37] that deacetylation increases the viscosity of certain xanthan solutions. For Xanthan C, the y-intercept value is 0.58, suggesting that deacetylation can lead to a viscosity decrease for some xanthans. Thus, the effects of deacetylation on viscosity appear to vary with the xanthan source. The molecular origin of this effect is not currently understood.

At first glance, Fig. 3 also seems to suggest that different xanthans exhibit different decay constants during stability studies. (Decay constant is inversely proportional to the slope of the first-order kinetic plot.) Even though all three xanthan solutions had an initial pH of 7.0, however, the pH dropped within 1 day at 120°C [248°F] and thereafter maintained values of 5.9, 5.5, and 4.7 for Xanthans B, C, and D, respectively. Because the decay constants for Xanthans B, C, and D were 22, 10, and 5 days, respectively, a relationship between pH and decay constant appears possible.

Numerous studies were conducted to establish the pH dependence of xanthan stability. All the studies involved solutions containing 1,500 ppm xanthan and salt concentrations of 0.567 eq/L. For most of the studies, the 0.567-eq/L salt concentration was achieved by using 3 wt% NaCl and 0.3 wt% $CaCl_2$. To attain pH values above 12, however, either 0.567*N* NaOH or 0.567*N* $Na_2S$ was used. Also, 500 ppm $Na_2S_2O_4$ was used as an oxygen scavenger, and dissolved oxygen levels were maintained at an undetectable level. For unbuffered solutions, pH values commonly dropped during the first day but were quite constant thereafter. Therefore, a time-averaged pH was calculated for each stability

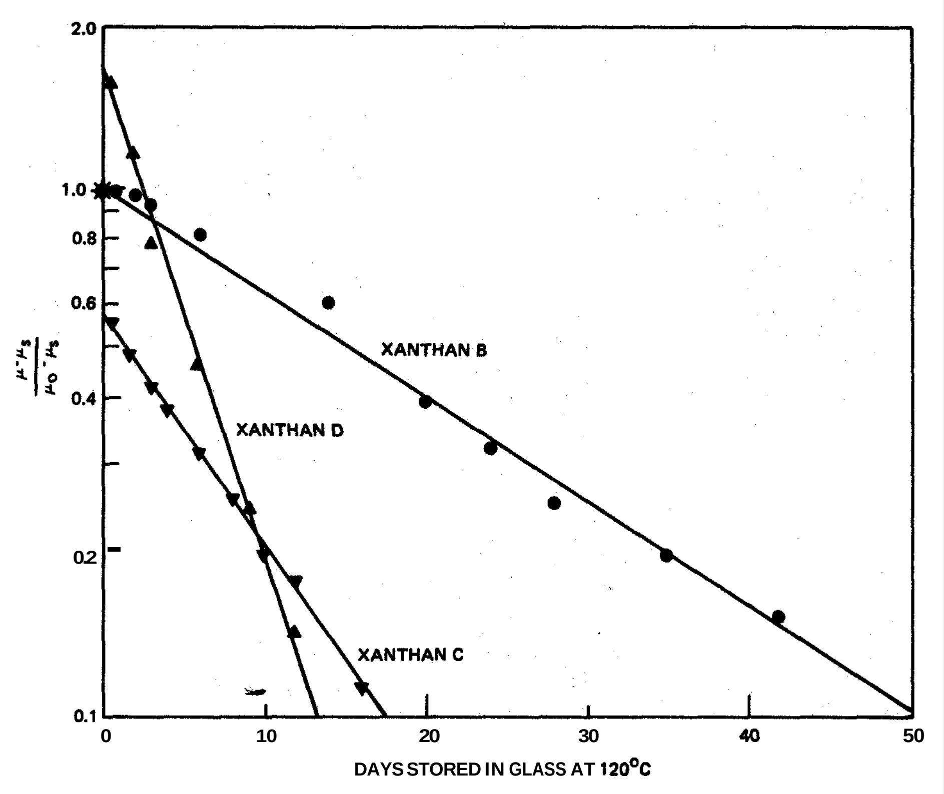

**Fig. 3—First-order kinetic plots: 1,500 ppm xanthan, 3% NaCl, 0.3% $CaCl_2$, 500 ppm $Na_2S_2O_4$, <2 ppb $O_2$, initial pH=7.0.**

study from the following equation:

$$\overline{\text{pH}}=[\Sigma(\text{pH}_i+\text{pH}_{i-1})(t_i-t_{i-1})]/[2\Sigma(t_i-t_{i-1})]. \quad \text{(8)}$$

As shown in Table 1 and Fig, 2, the time-averaged pH was close to the measured pH for all but the very first part of the experiment for temperatures at and above 96°C [205°F].

The dependence of the viscosity decay constant at 120°C [248°F] on the time-averaged pH is shown in Fig. 4. The maximum stability is observed between pH 7 and 8. Below pH 7, decay constants decrease significantly with decreasing pH. This suggests that acid-catalyzed hydrolysis may play an important role in xanthan degradation. Although fewer experiments were conducted in alkaline solutions, the available decay constants in Fig. 4 indicate that xanthan stability decreases above pH 8 as the solutions become more alkaline. This suggests that base-catalyzed fragmentation reactions can also play a role in xanthan degradation. The data in Fig. 4 can be fit reasonably well by use of the equation

$$\tau=1/(k_o+k_H[H^+]+k_{OH}[OH^-]), \quad \text{(9)}$$

where $k_H$ =rate constant for acid-catalyzed hydrolysis, $k_{OH}$ =rate constant for base-catalyzed fragmentation, and $k_o$ =rate constant associated with factors other than pH. At 120°C [248°F], the parameters used fork,, $k_H$, and $k_{OH}$ for the fit in Fig. 4 were 0.02 days–', 25 000 L/mol·d, and 1500 L/mol·d, respectively. A greater uncertainty exists in the value for $k_{OH}$ because of the data scatter observed around pH 9 in Fig. 4. For the fit shown, however, note that $k_H$ is about 17 times greater than $k_{OH}$. This difference is qualitatively consistent with expectations because glycosidic linkages between sugar units are known to be more susceptible to acid-catalyzed hydrolysis than to base-catalyzed reactions,[41]

Between pH 7 and 8, the combined contributions from acid-catalyzed hydrolysis and base-catalyzed fragmentation reactions are minimized so that $k_o$ dominates in the determination of the decay constant. At neutral pH, it is possible that water molecules and various anions (e.g., chloride) promote hydrolysis of glycosidic link-

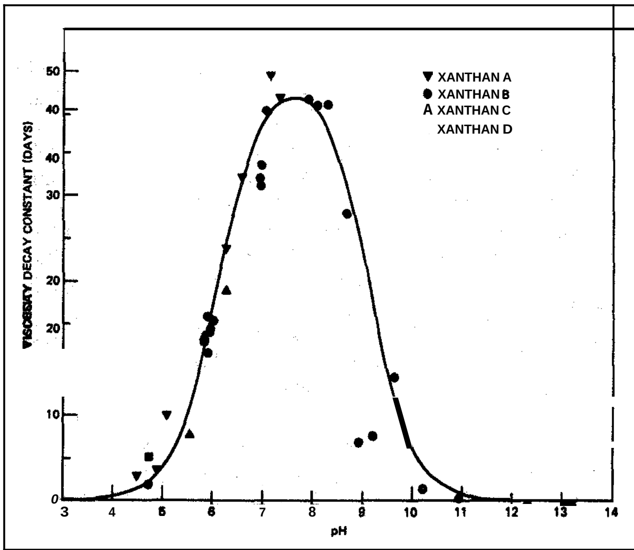

**Fig. 4—Effect of pH on xanthan stability at 120°C: 1,500 ppm xanthan, 500 ppm $Na_2S_2O_4$, <2 ppb $O_2$, salt normality =0.567 eq/L. Solid curve assumes that $\tau$=1/(0.02+25,000 [$H^+$]+1,500 [OH–]).**

**TABLE 2—EFFECT OF DISSOLVED OXYGEN ON XANTHAN STABILITY***

| Temperature (°C) | Viscosity Half-Life (days) <2 ppb $O_2$ | Viscosity Half-Life (days) 50 ppb $O_2$ |
|---|---|---|
| 64 | >1,000 | 225 |
| 80 | 500 | 33 |
| 96 | 70 | 15 |
| 120 | 5 | 1 |

*1,500 ppm Xanthan B, 3% NaCl, 0.3% $CaCl_2$, $\overline{\text{pH}}$=5, stored in glass.

**TABLE 3—EFFECTS OF REDUCING AGENTS, ANTIOXIDANTS, AND IRON**

| Entry | Xanthan* | Other Additives | pH | Viscosity Decay Constant at 120°C (days) |
|---|---|---|---|---|
| 1 | B | none | 7 | 13 |
| 2 | B | 500 ppm $Na_2S_2O_4$ | 7 | 45 |
| 3 | A | 500 ppm $Na_2S_2O_4$ | 7 | 46 |
| 4 | B | 800 ppm $Na_2SO_3$,<br>800 ppm $NaHCO_3$ | 7 | 37 |
| 5 | A | 800 ppm $Na_2SO_3$,<br>800 ppm $NaHCO_3$ | 7 | 38 |
| 6 | B | 800 ppm $Na_2SO_3$,<br>800 ppm $NaHCO_3$ | 8 | 46 |
| 7 | B | 1,500 ppm isopropanol,<br>750 ppm thiourea,<br>800 ppm $Na_2SO_3$,<br>800 ppm $NaHCO_3$ | 8 | 47 |
| 8 | A | 1,500 ppm isopropanol,<br>750 ppm thiourea,<br>800 ppm $Na_2SO_3$,<br>800 ppm $NaHCO_3$ | 8 | 47 |
| 9 | A | 500 ppm $Na_2SO_3$,<br>32 ppm $NaBH_4$ | 8 | 46 |
| 10 | B | 800 ppm $Na_2SO_3$ | 6 | 21 |
| 11 | B | 500 ppm $Na_2S_2O_4$ | 6 | 22 |
| 12 | B | 500 ppm $Na_2S_2O_4$,<br>50 ppm iron | 6 | 20 |

*1,500 ppm xanthan, 3% NaCl, 0.3% $CaCl_2$, <2 ppb $O_2$.

ages through nucleophilic substitution reactions.[43] Additional studies to test this hypothesis will be discussed shortly.

Included in Fig. 4 are results from tests involving xanthans from four different commercial sources. Interestingly, the decay constants appear to be more strongly dependent on the pH than on the commercial source.

**Effects of Reducing Agents, Antioxidants, and Iron.** Free-radical, oxidative/reductive reactions are thought to play a major role in xanthan degradation if dissolved oxygen is present.[29] Dissolved oxygen levels as low as 50 ppb can dramatically impair xanthan stability if antioxidant stabilizers are not added (see Table 2). If oxygen is not present, however, will free-radical reactions still constitute the dominant degradation mechanism, or will other types of mechanisms become more important? To address this question, a series of experiments were undertaken to test xanthan stability in the absence of dissolved oxygen but in the presence of certain reducing agents, antioxidants, and iron. Table 3 lists the results.

Entry 1 in Table 3 refers to a xanthan solution that was prepared without the use of an oxygen scavenger. Comparison reveals that the decay constant for Entry 1 is much less than those of Entries 2 through 5 in Table 3. There are at least two possible explanations why the presence of an oxygen scavenger may have improved xanthan stability. First, it is possible that, even though dissolved oxygen was undetectable (<2 ppb), some residual oxygen (probably part-per-trillion levels) could be left to attack xanthan when oxygen scavengers were not used. A second explanation involves an assumption that peroxides may be generated on the xanthan molecule because of extensive aeration during fermentation.[36] These peroxides are probably destroyed by the reducing action of the oxygen scavengers. If oxygen scavengers are not used, however, existing peroxides could degrade the polymer. No other evidence of reaction between xanthan and the oxygen scavengers was observed. In particular, the oxygen scavengers did not promote gelation.

Except for the first entry, all other entries in Table 3 involve use of an oxygen scavenger. When either $Na_2S_2O_4$ or $Na_2SO_3$ is used, similar decay constants are observed (for a given pH). Entries 6 through 8 in Table 3 reveal that addition of an isopropanol/thiourea antioxidant does not significantly change xanthan's decay constant if dissolved oxygen is not present. This observation was also reported by Ryles.[4] If free-radical, redox reactions were dominant, one would expect the addition of isopropanol and thiourea to increase the decay constant significantly.[29] Because the decay constants remained unchanged, these redox reactions appear to be less important than other types of reactions in xanthan degradation. This conclusion is applicable only for the case when dissolved oxygen is excluded.

Entries 11 and 12 in Table 3 provide additional evidence suggesting that redox reactions may not dominate the degradation process if oxygen is not present. In Entry 12, the solution was stored in a teflon-Coated, steel cylinder. (In all other entries, the solutions were stored in glass.) In spite of the teflon coating, 50 ppm of dissolved iron was detected in the solution shortly after the study began at 120°C [248°F]. Even so, this dissolved iron did not significantly change the decay constant. Presumably, the iron exists in solution as $Fe^{++}$. If $Fe^{+++}$ had been present, one would have expected a redox couple to be established that would have accelerated xanthan degradation.[29] Incidentally, note that the pH value was 6 for Entries 10 through 12. The lower pH explains why the decay constants for these entries were lower than those for Entries 2 through 9.

Note also that use of sodium borohydride (Entry 9) did not significantly change the decay constant. This reducing agent was proposed as a means of destroying peroxides in xanthan.[36] The results in Table 3 suggest that an oxygen scavenger may be equally effective in this role. Incidentally, tests were conducted to establish how much active oxygen (i.e., oxygen in peroxides) is present in xanthan. The test method involved dissolving the polymer in water, adding excess potassium iodide to the solution, and then titrating the released iodine with $Na_2S_2O_3$. Results revealed that no active oxygen was detected. Considering the detection limits of the test, the peroxide content of Xanthan B was determined to be < 17 ppm.

An analysis of degradation products would also be useful in distinguishing between hydrolysis and oxidation mechanisms. This activity is currently in progress using high-performance liquid chromatography and various wet chemistry techniques.

**Effects of Temperature, Salinity, and Ionic Character.** In planning a chemical flood, the engineer needs to estimate viscosity losses for the injected fluids as a function of time and temperature. Because xanthan degradation is a chemical reaction (or a sequence of chemical reactions), one must use kinetic concepts, such as decay and rate constants, activation energies, and Arrhenius graphs to characterize these viscosity losses. It is not correct to assume that because a polymer solution has maintained a certain viscosity for a few months or a year, it will maintain this viscosity indefinitely.

TABLE 4—XANTHAN STABILITY IN BRINE VS. IN DEIONIZED WATER*

| Temperature (°C) | Viscosity Decay Constant (days) In Deionized Water | Viscosity Decay Constant (days) In Brine 3% NaCl, 0.3% $CaCl_2$ |
|---|---|---|
| 64 | 40 | >1,000 |
| 80 | 2 | 700 |
| 96 | 0.6 | 100 |
| 120 | 0.1 | 7 |

*1,500 ppm Xanthan B, pH = 5, <2 ppb $O_2$, stored in glass.

TABLE 5—TEMPERATURE DEPENDENCE OF POLYMER STABILITY*

| Polymer | pH | Viscosity Decay Constant (days) at 96°C | Viscosity Decay Constant (days) at 120°C | Activation Energy (kJ/mol) |
|---|---|---|---|---|
| Xanthan A | 5 | 229 | 11 | 153 |
| Xanthan A | 7 | 475 | 46 | 117 |
| Xanthan B | 5 | 100 | 7 | 134 |
| Xanthan B | 7 | 360 | 45 | 104 |
| HEC | 6 | 11 | 0.6 | 146 |
| HEC | 7 | 46 | 4 | 123 |

*1,500 ppm xanthan or 3,000 ppm HEC, 3% NaCl, 0.3% $CaCl_2$, <2 ppb $O_2$, stored in glass.

An activation energy is found from the slope of an Arrhenius graph, which is a plot of the logarithm of the degradation rate constant vs. the reciprocal of the absolute temperature. If the elementary reaction steps are not known (as is the case for xanthan degradation), then empirical rate constants (e.g., the reciprocal of a viscosity decay constant) must be used to characterize the kinetics. Thus, if decay constants $\tau_1$ and $\tau_2$ are known for the temperatures $T_1$ and $T_2$, respectively, then an activation energy, $E_a$, can be estimated:

$$E_a = R[\ln(\tau_2/\tau_1)]/(T_2^{-1} - T_1^{-1}), \quad \text{.....................} (10)$$

where $R$ = gas constant. Of course, because details of the molecular kinetics of xanthan degradation are not known, the activation energy that is calculated with Eq. 10 is not necessarily associated with a particular elementary reaction. Instead, this $E_a$ value is simply a constant that characterizes the temperature dependence of xanthan degradation, which is of more interest to the engineer planning a chemical flood.

Arrhenius graphs and calculations can be very useful in estimating the limits of polymer stability. For example, if polymer degradation can be characterized by a constant activation energy over a temperature range, then decay constants measured at the high end of this temperature range can be used along with Eq. 10 to predict decay constants at the lower end of the range. This procedure could be particularly valuable in chemical floods where the polymer must remain stable for many years at the reservoir temperature. From a few studies at temperatures above reservoir temperature, enough data can be collected in a relatively short time so that an Arrhenius calculation could be used to estimate the decay constant at reservoir temperature. Of course, care must be taken to avoid pitfalls when an Arrhenius analysis is used. In particular, predictions can be erroneous if the activation energy is not constant in the temperature range over which the Arrhenius analysis is being applied.

If the Arrhenius analysis is not used, then one would have to conduct a stability study at reservoir temperature that would last a very long time to ensure that the polymer was sufficiently stable. Depending on the specific chemical flood and reservoir, this stability study might require 5 or 10 years or even longer to complete.

The temperature dependence of degradation is shown in Table 4 for xanthan in a 3.3 wt% total dissolved solids (TDS) brine and in deionized water. (Because of the counter-ions associated with xanthan, there will still be a low level of alkali metal ions—about 100 ppm—in the solutions that were prepared with deionized water.) Xanthan is clearly much more stable in saline solutions than in deionized water.

The greater stability observed in saline solutions is thought to be associated with the nature of the helix/coil transition.[27] In deionized water, xanthan exists in the disordered, coil conformation at elevated temperatures; glycosidic linkages, therefore, may be easily accessible for chemical attack. In contrast, xanthan is more likely to exist in the helical conformation in saline solutions, so the polymer backbone may be more protected. Because the melting temperature varies with salinity (see Eqs. 1 through 3), it is conceivable that in a given brine, xanthan could be dramatically less stable above $T_m$ than below $T_m$.[38,40] If this is true, a sharp change in the activation energy for xanthan degradation should be observed as the temperature is raised above $T_m$. For example, Clarke-Sturman[40] reported data for xanthan degradation in 5% HCl in which the activation energy increased by a factor of two as temperature was raised through the melting temperature of 115°C [239°F]. If one uses only the stability data in the vicinity of $T_m$, then an Arrhenius analysis would predict xanthan stability at lower temperatures to be much greater than is observed experimentally. This error emphasizes the importance of having a valid activation energy when the Arrhenius analysis is conducted.

When Eq. 10 and the data in Table 4 are used, the activation energy for xanthan degradation in the 3.3% TDS brine is found to be the same (132 to 134 kJ/mol [125 to 127 Btu/mol]) between 80 and 96°C [176 and 205°F] as it is between 96 and 120°C [205 and 248°F]. Thus, the Arrhenius analysis should be valid between 80 and 120°C [176 and 248°F]—at least for this xanthan in the 3.3% TDS brine at pH 5. Also, because the activation energy is constant, one would suspect that the melting temperature under these conditions does not fall within the range from 80 to 120°C [176 to 248°F]. This speculation is consistent with the studies of Holzwarth,[25] who noted that the presence of calcium dramatically raises $T_m$. As mentioned earlier, the presence of 0.3% $CaCl_2$ in the brine could increase $T_m$ to about 200°C [392°F].

Table 5 lists results of additional studies of the temperature dependence of degradation. For both Xanthans A and B, the activation energy is 30% higher at pH 5 than at pH 7. Thus, caution should be exercised when data collected at one pH are used to estimate viscosity losses at another pH. Table 5 also reveals that different xanthans can show slightly different activation energies. Both at pH 5 and 7, the activation energy for Xanthan A is 12 to 14% higher than that for Xanthan B. This difference may be connected to the different pyruvate contents of the polymers. (The degree of pyruvation on side chains is 70% for Xanthan A and 39% for Xanthan B.)

If Eq. 10 is used with the data in Table 5 to estimate polymer stabilities at lower temperatures, 5-year viscosity half-lives are predicted to occur at 80 and 76°C [176 and 169°F] for Xanthans A and B, respectively, at pH 7. These predictions require that $E_a$ be fairly constant between 75 and 120°C [167 and 248°F]. We note that Clarke-Sturman[40] has projected that xanthan solutions at neutral pH may exhibit a viscosity half-life in excess of 3 years at 90°C [194°F]. Our data suggest that the viscosity half-life will be just under 2 years at 90°C [194°F] for Xanthan A. Two factors stand out as possible explanations for the different projections. The most likely factor is that our studies were conducted at pH 7, whereas Clark-Sturman's projection for stability at pH 7 was based on experiments that were performed in 5% HCl (pH 0). As mentioned earlier, caution must be used when predicting stabilities at pH values that differ substantially from the pH at which the data were collected. A second possible explanation may be differences in the xanthan samples that were used in the two laboratories.

Table 5 also includes data for degradation of hydroxyethylcellulose (HEC). In light of the findings of Clarke-Sturman,[40] the HEC data provide further evidence that Xanthans A and B are in the helical conformation at 120°C [248°F]. Clarke-Sturman noted that below $T_m$, xanthan degradation proceeded 25 times slower than HEC degradation, but the activation energies exhibited by the two polymer types were roughly the same. Xanthan and HEC both have the same $\beta$(1-4) linked backbone, but HEC is thought to exist always as a random coil. It is expected that xanthan stability should

### TABLE 6—EFFECT OF SALINITY ON XANTHAN STABILITY AT 120°C*

| NaCl Concentration (*N*) | Viscosity Decay Constant at 120°C (days) | $T_m$ from Eq. 1 |
|---|---|---|
| 0.1417 | 10 | 97 |
| 0.2835 | 12** | 106 |
| 0.567 | 42 | 115 |
| 1.134 | 39 | 124 |
| 2.268 | 44 | 133 |

*1,500 ppm Xanthan B, 500 ppm $Na_2S_2O_4$, <2 ppb $O_2$, $\overline{pH}$ = 7, stored in glass at 120°C.

**Decay curve was not characterized well by a single decay constant. See text.

### TABLE 7—EFFECT OF IONIC CHARACTER ON XANTHAN STABILITY*

| Brine | Viscosity Decay Constant at 120°C (days) |
|---|---|
| 0.567 *N* NaCl | 42 |
| 0.567 *N* NaCl** | 42 |
| 0.567 *N* KCl** | 57 |
| 0.567 *N* $CaCl_2$** | 10 |
| 0.567 *N* $MgCl_2$** | 11 |
| 0.567 *N* NaF | 43 |
| 0.567 *N* NaBr | 14† |
| 0.567 *N* NaI | 12† |
| 0.567 *N* $Na_2SO_4$ | 59 |

*1,500 ppm Xanthan B, 500 ppm $Na_2S_2O_4$, $\overline{pH}$ = 7, <2 ppb $O_2$, stored in glass at 120°C.

**Samples contained 10 g of $CaCO_3$ solid that buffered the solutions at pH 7 throughout the experiments. The other samples were not buffered and had an initial pH of 8 and a time average of 7 because of the pH drop that occurred during the first day at 120°C.

†Viscosity-loss curves were not characterized well by a single exponential. See text.

approach that of HEC as the temperature is raised above $T_m$ where xanthan also exists in a disordered conformation.[40] From the data in Table 5 it is evident that the stabilities of xanthan and HEC are no more similar at 120°C [248°F] than at 96°C [205°F], suggesting that the xanthans are still in the ordered conformation at 120°C [248°F].

To investigate the role of the helix/coil transition further, xanthan stability studies were performed at 120°C [248°F] with five solutions that ranged in NaCl concentration from 0.1417 to 2.268 N. Table 6 shows the results. Also included in Table 6 are $T_m$ values that were calculated for each salinity with Eq. 1. For NaCl concentrations of 0.567 N and higher, the viscosity decay constants at 120°C [248°F] are approximately 40 days—similar to the value observed in the 3.3% TDS brine. For the 0.1417 N NaCl solution, the decay constant is only 10 days, confirming that the polymer is less stable when the temperature is significantly above $T_m$. For xanthan in 0.2835 N NaCl, a decay constant of 12 days was obtained from the linear regression, but the data are not characterized well by a single exponential. From 0 to 20 days at 120°C [248°F], the viscosity losses were identical to those observed for the solutions with higher salinities. Thereafter, however, the viscosity dropped much more rapidly than would be predicted from an exponential decay. Measurements confirmed that no oxygen had leaked into the storage container. Perhaps xanthan remained as a metastable helix for the first 20 days in the 0.2835 N NaCl solution, but thereafter denatured into the less stable coil conformation.

Several experiments also were conducted to investigate the effects of ionic character on xanthan stability. These studies were all conducted at 120°C [248°F] with a constant normality (0.567 N salt in addition to the polymer and oxygen scavenger). Table 7 lists the results. Xanthan was found to be significantly less stable in solutions with 0.567 N $CaCl_2$ or $MgCl_2$ than in solutions with 0.567 N NaCl or KCl. This was unexpected because Eq. 3 predicts $T_m$ to be far above 120°C [248°F] for the divalent cation solutions. Perhaps high concentrations of divalent cations actually destabilize the xanthan helix, in contrast to the effect found at low divalent cation concentrations.

Several experiments were performed with various anions to examine the role of nucleophilic substitution in xanthan degradation. Presumably, if nucleophilic substitution is important, xanthan degradation should be affected by the presence of stronger nucleophiles. The following anions are listed in increasing order of nucleophilic strength[43]: $F^- \ll Cl^- < Br^- < I^-$.

Table 7 shows the effects of various anions on xanthan stability. In the presence of 0.567 N NaF or $Na_2SO_4$, xanthan stabilities were no less than those in 0.567 N NaCl. In brines containing 0.567 N NaBr or NaI, the polymer was less stable, and the viscosity-loss curves were not characterized well by a single exponential. Like the behavior found in 0.2835 N NaCl at 120°C [248°F], the viscosity-loss curves matched those for 0.567 N NaCl between 0 and 20 days. Thereafter, the viscosity dropped much more rapidly than would be predicted from an exponential decay.

Xanthan is more stable in the fluoride brine than in the iodide brine. However, xanthan stability in the iodide brine is not significantly different from that in the bromide brine. Thus, xanthan degradation in the presence of stronger nucleophiles failed to follow the same order of the anion's nucleophilic strength. Additional experiments will be needed to clarify the role of nucleophilic substitution in xanthan degradation.

**Effects** of Buffers and Contact With **Rock.** Because of the pH drop experienced by unbuffered xanthan solutions, several experiments were performed with chemical buffers. These buffers included phosphate, tris, imidazol, and hepes. Table 8 lists many of the results. In all cases, the buffers were very effective at maintaining the pH at a value of 7.0. At 96°C [205°F], the viscosity decay constants observed in the buffered solutions were generally not greatly different from those found in the unbuffered 3.3% TDS brine (360 days for Xanthan B). However, at 120°C [248°F], the chemical buffers seemed to impair xanthan stability. In the presence of 0.567 N phosphate, tris, imidazol, or hepes, the decay constants at 120°C [248°F] were 20 to 100 times faster than those observed in the 3.3% TDS brine. For solutions that contained both 0.567 N buffer and the salts in the 3.3% TDS brine, xanthan stability at 120°C [248°F] was improved but was still less than that found when no buffer was used. Even low concentrations of tris (0.004 *N*) appear to impair xanthan stability in the 3.3% TDS brine at 120°C [248°F]. Perhaps the buffers destabilize xanthan's helical structure at high temperatures.

In a reservoir, the rock minerals act to buffer solutions. Therefore, it seems worthwhile to examine polymer stability in the pres-

### TABLE 8—EFFECT OF BUFFERS ON XANTHAN STABILITY*

| Brine | Viscosity Decay Constant (days) at 96°C | Viscosity Decay Constant (days) at 120°C |
|---|---|---|
| 0.567 *N* $NaH_2PO_4/Na_2HPO_4$ | 420 | 2.0 |
| 0.567 *N* TRIS | 280 | 1.2 |
| 0.567 *N* imidazol | 204 | 0.3 |
| 0.567 *N* HEPES | 425 | 0.4 |
| 3% NaCl, 0.3% $CaCl_2$, no buffers or rock added | 360 | 45 |
| 3% NaCl, 0.3% $CaCl_2$, 0.004 *N* TRIS | — | 12 |
| 3% NaCl, 0.3% $CaCl_2$, 0.567 *N* TRIS | 445 | 21 |
| 3% NaCl, 0.3% $CaCl_2$, 0.567 *N* imidazole | 313 | 15 |
| 3% NaCl, 0.3% $CaCl_2$, 0.567 *N* HEPES | — | 33 |
| 3% NaCl, 0.3% $CaCl_2$, 40 g $CaCO_3$ powder | 327 | 46 |

*1,500 ppm Xanthan B, 500 ppm $Na_2S_2O_4$, pH = 7, <2 ppb $O_2$, stored in glass.

ence of these minerals. Table 8 includes results of stability studies that were conducted in the presence of powdered calcium carbonate (40 g **$CaCO_3$/200** mL solution). (Before the experiment was started, the calcium carbonate was washed with a separate xanthan solution to satisfy adsorption requirements by the solid.) Both at % and 120°C [205 and **248°F]**, the pH was maintained at a value of 7 throughout the experiment—no initial pH drop was noted. Also, at both temperatures, the viscosity decay constants were similar to those found for unbuffered solutions involving the 3.3% TDS brine that had a pH value of 7. Thus, it appears that contact with calcium carbonate may be a useful method to buffer solutions during stability studies.

## implications in EOR

Very few reports have been published that address the question of how long a polymer must be stable during a chemical flood. Well spacing and injection rates should be key factors in determining the stability requirements. With an injection rate of **5** B/D-ft [2.6 $m^3/d \cdot m$] of pay, the residence time of an injected polymer solution may be 15 to 20 years for an 8-ha [20-acre] well spacing, but could be around **5** years for a well spacing of 2 ha [5 acres].

The stability requirements may also vary depending on reservoir heterogeneity and the **type** of chemical **flood** being applied. Clifford and **Sorbie**[46,47] simulated the performance of a polymer flood in a high-permeability, heterogeneous reservoir. They predicted that vertical crossflow will lead to recovery of surprisingly high levels of incremental oil even though the viscosity half-life of the injected polymer solution may be only 1 year. In contrast, there are many circumstances where long viscosity half-lives will be essential. For example, in a surfactant flood, mobility control must be maintained for a significant fraction of the project life. If mobility control is **lost (i**. e., the polymer degrades), the injected chemical banks will lose viscosity and finger through the oil bank. Because the ultimate recovery projected for surfactant flooding is about seven times that projected for polymer flooding,[48] a significant need exists for a polymer that will provide viscosity half-lives of **5** to 10 years or more at elevated temperatures.

The data and Arrhenius analyses reported in this paper suggest that under ideal conditions (no dissolved oxygen, pH 7 to 8, and moderate to high salinities), solutions made from existing xanthans may exhibit viscosity half-lives of **5** years at temperatures between 75 and 80°C [167 and 176°F]. To the best of our knowledge, no stability experiments have lasted for **5** years or more at these temperatures. Thus, confirmation or disproval of the Arrhenius predictions must await the results of some very-long-term tests. In the meantime, it may be unwise to assume that xanthan will be sufficiently stable to provide viscosity half-lives of **5** years or longer at temperatures above 75 to 80°C [167 to 176°F].

If conditions are not ideal, then xanthan may be considerably less stable. As Table 2 illustrated, introduction of only **50** ppb of dissolved oxygen can reduce the viscosity half-life by a factor of five or more. This result emphasizes the importance of excluding all dissolved oxygen from the injected polymer solution and/or of using antioxidants to stabilize the polymer. Also, xanthan stability will decrease if the pH is less than 7 or greater than 8. Thus, it is important to know the pH of the injected fluids and of the reservoir fluids. In addition, the low stability of xanthan under high-temperature, high-pH conditions brings into question the utility of the polymer during hot alkaline floods.

We hope that **this** paper will stimulate more productive efforts to improve polysaccharide stability. Although reducing agents and antioxidants may be essential in protecting the polymer from oxidation, they will probably not significantly improve xanthan stability beyond a certain point. This is because degradation mechanisms other than oxidation become dominant once the oxidizing agents have been deactivated. Thus, a significant improvement in xanthan stability is more likely to come from efforts to protect the polymer backbone from hydrolysis rather than from efforts to develop a better antioxidant. Even **so**, making xanthan more resistant to hydrolysis will be a very challenging task.

## Conclusions

We find that in the absence of dissolved oxygen, xanthan solutions exhibit their maximum stability at pH values between 7 and 8. Below pH 7, viscosity decay constants decrease significantly with decreasing pH, indicating that acid-catalyzed hydrolysis may have an important role in xanthan degradation. Xanthan stability also drops sharply above pH 8 as solutions become more alkaline, suggesting that base-catalyzed fragmentation reactions may also **be** important.

The presence of only **50** ppb of dissolved oxygen can reduce viscosity half-lives by a factor of five or more from those observed in the absence of dissolved oxygen. Thus, use of reducing agents and/or antioxidants can be desirable to minimize the role of free-radical, oxidative/reductive reactions if dissolved oxygen cannot be excluded. However, if common oxygen scavengers can main**tain** the dissolved oxygen content at undetectable levels (<2 ppb), then antioxidant packages (such **as** thiourea and isopropanol) and reducing agents (such **as** sodium borohydride) have no further effect on xanthan stability. This observation suggests that in the absence of dissolved oxygen and other oxidizing agents, oxidation/reduction reactions are not the dominant mechanism for xanthan degradation.

Viscosity decay constants for xanthan solutions were found to vary both with salinity and ionic character. As reported earlier, xan**than stability was found** to be greatest at higher salinities, where the **polymer is thought to** be in a helical conformation that provides protection from chemical attack. For xanthan in a brine containing 3% NaCl and 0.3% $CaCl_2$, stability data coupled with literature values for xanthan melting temperatures indicate that the polymer is in the helical conformation for temperatures ≤ 120°C **[248°F].**

Data collected at different elevated temperatures were used with an Arrhenius analysis to estimate viscosity half-lives **as** a function of temperature for xanthan solutions. The analysis indicates that under ideal conditions (no dissolved oxygen, pH 7 to 8, moderate to high salinities), a xanthan solution could maintain at least half of its original viscosity for a period of **5** years if the temperature does not exceed 75 to 80°C [167 to 176°F]. Of course, if conditions are not ideal, then xanthan solutions can be considerably less stable.

In many chemical floods, viscosity half-lives of **5** years or more will be needed to maintain mobility control. In view of the potential for application of chemical floods in the warmer reservoirs, a significant need exists for polymers that will be more stable and effective at elevated temperatures.

## Nomenclature

$E_a$ = activation energy, J/mol [Btu/mol]
$k_H$ = rate constant for acid-catalyzed hydrolysis, **days**$^{-1}$
k, = rate constant for effects not associated with pH, L/mol·d
$k_{OH}$ = rate constant for base-catalyzed fragmentation, L/mol·d
$M_n$ = number-averaged molecular weight, daltons
$M_w$ = weight-averaged molecular weight, daltons
$\overline{pH}$ = time-averaged pH
r = correlation coefficient
R = gas constant, 8.3143 J/mol·K
$t$ = time, days
T = temperature, K [°F]
$T_m$ = "melting" or transition **temperature, °C [°F]**
$\mu$ = solution viscosity, mPa·s [cp]
$\mu_o$ = initial solution viscosity, mPa·s [cp]
$\mu_s$ = solvent viscosity, mPa·s [cp]
7 = viscosity decay constant, days

## Acknowledgments

We thank T.L. Ashcraft, G. Holzwarth, and L.D. Talley for helpful discussions. We also acknowledge the help of Michael Tran in performing some of the stability tests, E.A. Lange in examining solutions for microbial growth, and K.K. Chokshi and R.A. Nadkarni for investigating the peroxide content of xanthan samples.

## References

1. Carey, B.S.: "1984 EOR Data Base," Exxon Production Research Co., for Natl. Petroleum Council, Washington, DC (1984).
2. Davison, P. and Mentzer, E.: "Polymer Flooding in North Sea Reservoirs," *SPEJ* (June 1982) 353–62.
3. Zaitoun, A. and Potie, B.: "Limiting Conditions for Use of Hydrolyzed Polyacrylamides in Brines Containing Divalent Ions," paper SPE 11785 presented at the 1983 SPE Intl. Symposium on Oilfield and Geothermal chemistry, Denver, June 1–3.
4. Ryles, R.G.: "Chemical Stability Limits of Water-Soluble Polymers Used," paper SPE 13585 presented at the 1985 SPE Intl. Symposium on Oilfield and Geothermal Chemistry, Phoenix, April 9–11.
5. Muller, G.: "Thermal Stability of High-Molecular-Weight Polyacrylamide Aqueous Solutions," *Polymer Bulletin* (1981) 5, 31–37.
6. Shupe, R.D.: "Chemical Stability of Polyacrylamide Polymers," *JPT* (Aug. 1981) 1513–29.
7. Jansson, P.E., Kenne, L., and Lindberg, B.: "Structure of the Extracellular Polysaccharide from *Xanthomonas campestris*," *Carbohydrate Research* (1975) 45, 275–82.
8. Orentas, D.G., Sloneker, J.H., and Jeanes, A.: "Pyruvic Acid Content and Constituent Sugars of Exocellular Polysaccharides from Different Species of the Genus *Xanthomonas*," *Cdn. J. Microbiol.* (1963) 9, 427–30.
9. Wernau, W.C.: "*Xanthomonas* Biopolymer for Use in Displacement of Oil from Partially Depleted Reservoirs," U.S. Patent No. 4,296,203 (1981).
10. Phillips, J.C. *et al.*: "A High-Pyruvate Xanthan for EOR," *SPEJ* (Aug. 1985) 594–602.
11. Lecourtier, J. *et al.*: "Rheological Properties of Simple and Double Helix Xanthan Solutions," paper MBTD 84 presented at the 1985 ACS Natl. Meeting, Chicago, IL, Sept. 8–13.
12. Dintzis, F.R., Babcock, G.E., and Tobin, R.: "Studies on Dilute Solutions and Dispersions of the Polysaccharide from *Xanthomonas campestris* NRRL B-1459," *Carbohydrate Res.* (1970) 13, 257–67.
13. Holzwarth, G.: "Molecular Weight of Xanthan Polysaccharide," *Carbohydrate Res.* (1978) 66, 173–86.
14. Whitcomb, P.G. and Macoska, C.W.: "Rheology of Xanthan Gum," J. *Rheology* (1978) 22, 493–04.
15. Wellington, S.L.: "Xanthan Gum Molecular Size Distribution and Configuration," *ACS Polymer Preprints* (1981) 22, No. 2.
16. Rinaudo, M. and Milas, M.: "Polyelectrolyte Behavior of a Bacterial Polysaccharide from *Xanthomonas campestris*," *Biopolymers* (1978) 17, 2663–78.
17. Holzwarth, G. and Prestridge, E.B.: "Multistranded Helix in Xanthan Polysaccharide," *Science* (1977) 197, 757–59.
18. Moorhouse, R., Walkinshaw, M.D., and Amott, S.: "Xanthan Gum—Molecular Conformation and Interactions," *Extracellular Microbial Polysaccharides,* Symposium Series, American Chem. Soc., Washington, DC (1977) No. 45, 90–102.
19. Holzwarth, G.M.: "Is Xanthan a Wormlike Chain or a Rigid Rod?" *Solution Properties of Polysaccharides,* Symposium Series, American Chem. Soc., Washington, DC (1981) No. 150, 15–23.
20. Southwick, J.G., Jamieson, A.M., and Blackwell, J.: "Quasi-Elastic Light Scattering Studies of Semidilute Xanthan Solutions," *Macromolecule*(1981) 14, 1728–32.
21. Muller, G. *et al.*: "Conformation of the Xanthan Molecule in an Ordered Structure," *Makromol. Chem., Rapid Commun.* (1984) 5, 203–08.
22. Sato, T. *et al.*: "Double-Stranded Helix of Xanthan in Dilute Solution: Further Evidence," *Polymer J.* (1984) 16, 423–29.
23. Sato, T., Norisuye, T., and Fujita, H.: "Double-Stranded Helix of Xanthan in Dilute Solution: Evidence from Light Scattering," *Polymer J.* (1984) 16, 341–50.
24. Milas, M. and Rinaudo, M.: "On the Existence of Two Different Secondary Structures for the Xanthan in Aqueous Solutions," *Polymer Bulletin* (1984) 12, 507–14.
25. Holzwarth, G.: "Conformation of the Extracellular Polysaccharide of *Xanthomonas campesnis*," *Biochemistry* (1976) 15, 4333–39.
26. Milas, M. and Rinaudo, M.: "Conformational Investigation of the Bacterial Polysaccharide Xanthan," *Carbohydrate Res.* (1979) 76, 189–%.
27. Lambert, F., Milas, M., and Rinaudo, M.: "Structure and Properties of a Polysaccharide Used in Enhanced Oil Recovery: Xanthan," *Proc.*, Assn. Rech. Tech. Exploit. Petrol. Enhanced Oil Recovery European Symposium, Paris (Nov. 8–10, 1982) 79–86.
28. Holzwarth, G. and Ogletree, J.: "Pyruvate-free Xanthan," *Carbohydrate Res.* (1979) 76, 277–80.
29. Wellington, S.L.: "Biopolymer Solution Viscosity Stabilization—Polymer Degradation and Antioxidant Use," *SPEJ* (Dec. 1983) 901–12.
30. Harris, M.J., Herp, A., and Pigman, W.: "Depolymerization of Polysaccharides Through the Generation of Free Radicals at a Platinum Surface," *Arch. Biochem. Biophys.* (1971) 142, 615–22.
31. Gilbert, B.C., King, C.M., and Thomas, C.B.: "The Oxidation of Some Polysaccharides by the Hydroxyl Radical," *Carbohydrate Res.* (1984) 125, 217–35.
32. Abdo, M.K.: "Waterflood Oil Recovery Process Employing Stabilized Biopolymers," U.S. Patent No. 4,141,842 (1979).
33. Shay, L.K. and Reiter, S.E.: "Amine Treatment of Polysaccharide Solution," U.S. Patent No. 4,485,020 (1984).
34. Glass, J.E.: "Treatment of Water Thickened Systems," U.S. Patent No. 4,486,340 (1984).
35. Sandell, L.S.: "Stabilization of Thickened Aqueous Fluids," U.S. Patent No. 4,486,317 (1984).
36. Philips, J.C. and Tate, B.E.: "Stabilizing Polysaccharide Solutions for Tertiary Oil Recovery at Elevated Temperature with Borohydride," U.S. Patent No. 4,458,753 (1984).
37. Jeanes, A., Pittsley, J.E., and Senti, F.R.: "Polysaccharide B-1459," *J. Appl. Polymer Sci.* (1961) 5, 519–26.
38. Ash, S.G. *et al.*: "Chemical Stability of Biopolymers," paper SPE 12085 presented at the 1983 SPE Annual Technical Conference and Exhibition, San Francisco, Oct. 5–8.
39. McNeely, W.H. and Kang, K.S. "Xanthan and Some Other Biosynthetic Gums," Industrial Gums, second edition, R.L. Whistler (ed.), Academic Press, New York City (1973) 473–97.
40. Clarke-Sturman, A.J.: "Hydrolytic Stability of Xanthan," paper MBTD 88 presented at the 1985 ACS Natl. Meeting, Chicago, IL, Sept. 8–13.
41. Aspinall, G.O.: "Chemical Characterization and Structure Determination of Polysaccharides," *The Polysaccharides,* Academic Press, New York City (1982) 1, 35–131.
42. BeMiller, J.N.: "Acid-Catalyzed Hydrolysis of Glycosides," *Adv. Carbohydrate Chem.* (1967) 22, 25–108.
43. Morrison, R.T. and Boyd, R.N.: *Organic Chemistry,* fourth edition, Allyn and Bacon, Boston, MA (1983) 204–58.
44. Seright, R.S. and Henrici, B.J.: "Xanthan Stability at Elevated Temperatures," paper SPE 14946 presented at the 1986 SPE Symposium on Enhanced Oil Recovery, Tulsa, April 20–23.
45. Miron, R.L.: "Removal of Aqueous Oxygen by Chemical Means in Oil Production Operations," *Materials Performance* (June 1981) 45–50.
46. Clifford, P.J. and Sorbie, K.S.: "Polymer Flooding in Stratified Systems: Recovery Mechanisms and the Effect of Chemical Degradation," paper presented at the 1984 IEA Collaborative Project on EOR, Trondheim, Norway, Oct. 4–5.
47. Clifford P.J. and Sorbie, K.S.: "The Effects of Chemical Degradation on Polymer Flooding," paper SPE 13586 presented at the 1985 SPE Intl. Symposium on Oilfield and Geothermal Chemistry, Phoenix, April 9–11.
48. *Enhanced Oil Recovery,* Natl. Petroleum Council, Washington, DC (1984) 62.

## SI Metric Conversion Factors

cp × 1.0* E−03 = Pa·s
°F (°F−32)/1.8 = °C

*Conversion factor is exact.

**SPERE**

Original SPE manuscript received for review April 20, 1986. Paper accepted for publication Aug. 12, 1988. Revised manuscript received Jan. 30, 1989. Paper (SPE 14946) first presented at the 1986 SPE/DOE Symposium on Enhanced Oil Recovery held in Tulsa, April 20–23.